Electrochimica Acta 540 (2025) 147177

Contents lists available at ScienceDirect

Electrochimica Acta

journal homepage: www.journals.elsevier.com/electrochimica-acta

Molecularly imprinted polymer-based sensor for the determination of 2,4-dinitrophenol in food supplements

Ricarda Torre [a], Patrícia Rebelo [a], Isabel Seguro [a], João G. Pacheco [a,*], Joana S. Amaral [b,c], Henri P.A. Nouws [a], Cristina Delerue-Matos [a]

[a] REQUIMTE/LAQV, Instituto Superior de Engenharia do Porto, Instituto Politécnico do Porto, Rua Dr. António Bernardino de Almeida 431, 4249-015 Porto, Portugal
[b] Centro de Investigação de Montanha (CIMO), Instituto Politécnico de Bragança, Campus de Santa Apolónia, 5300-253 Bragança, Portugal
[c] Laboratório Associado para a Sustentabilidade e Tecnologia em Regiões de Montanha (SusTEC), Instituto Politécnico de Bragança, Campus de Santa Apolónia, 5300-253 Bragança, Portugal

ARTICLE INFO

Keywords:
2,4-Dinitrophenol
Molecularly Imprinted Polymer
Paper-based transducer
Electrochemical sensor
Food supplements

ABSTRACT

The rising demand for weight-loss solutions, driven by obesity concerns and societal pressure, has led to an increasing growth in both the consumption and market of food supplements. However, several studies have identified food supplements as common targets of economically motivated adulteration by the addition of pharmaceutical drugs to enhance the product's effects. Despite its toxicity and associated health risks, 2,4-dinitrophenol (2,4-DNP) is prone to be illegally added to weight-loss products due to its thermogenic effect, emphasizing the need for reliable detection methods. In this study, we report the first electrochemical sensor integrating a molecularly imprinted polymer (MIP) onto a paper-based platform for the selective detection of 2,4-DNP. This innovative approach combines the high selectivity of MIPs with the cost-effectiveness, portability, and disposability of paper-based devices, paving the way for practical, on-site monitoring of 2,4-DNP in food supplements. The sensor features a paper-based transducer with a gold and carbon ink working electrode that was modified with the MIP, which was synthesized through precipitation polymerization. The sensor's performance was thoroughly evaluated, demonstrating a linear range of 50 - 1000 μmol L^{-1} and a limit of detection of 16.3 μmol L^{-1}. The sensor was successfully applied to the analysis of various commercially available weight-loss food supplements (e.g., slimming activators, fat burners, thermoshape) in capsule form, yielding satisfactory recoveries ranging from 85 to 109%. These results highlight the potential of this MIP-based sensor for the rapid, sensitive, and selective determination of 2,4-DNP in food supplements, contributing to consumer safety and regulatory compliance.

1. Introduction

In the last decades, the prevalence of overweight and obesity has been rising, particularly in Western developed countries, leading to increasing dissatisfaction with physical appearance. The growing concerns over obesity and societal pressures towards a slim figure, have driven a rising demand for weight-loss solutions [1]. Among those, several consumers look for quick and easy approaches while avoiding making lifestyle changes, such as diet and exercise. This has contributed to the increasing growth of the food supplements market, with popular products, known as "fat burners," typically containing ingredients that boost metabolism, such as caffeine, green tea extract, and carnitine [2]. Moreover, because most food supplements include medicinal plants as ingredients, they are frequently advertised as "natural" products, which can mislead consumers in perceiving these products as safer than conventional pharmaceuticals [3]. Despite including medicinal plants, food supplements are legally considered foods according to Directive 2002/46/EC [4] and the Dietary Supplement Health and Education Act [5]. Therefore, they do not require any specific risk assessment before being commercialized, with the responsibility for food safety issues relying on food business operators. Although manufacturers do not have to provide evidence that supports the product's safety and effectiveness, food supplements must be safe, effective, and absent from adulterations. Nevertheless, several studies have reported the detection of pharmaceutical drugs illegally added to food supplements to boost their effect, aiming for increasing sales and higher economic gain. In particular,

* Corresponding author.
E-mail address: jpgpa@isep.ipp.pt (J.G. Pacheco).

https://doi.org/10.1016/j.electacta.2025.147177
Received 14 June 2025; Received in revised form 11 August 2025; Accepted 16 August 2025
Available online 16 August 2025

different substances have been detected in supplements for weight loss including banned anorexics such as sibutramine and rimonabant, banned laxatives such as phenolphthalein, amphetamine-derived drugs such as fenproporex, and antidepressants such as fluoxetine [6–8]. Recently, Amidžic et al. [9], conducted a review of data reports spanning from 2011 to 2022 of the Rapid Alert System for Food and Feed (RASFF), concluding that among the unauthorized pharmaceuticals identified in food supplements for weight loss, 45 were related to sibutramine, 18 to phenolphthalein, 7 to *N*-didesmethyl sibutramine and 6 related to 2, 4-dinitrophenol (2,4-DNP). 2,4-DNP is a crystalline solid that is only slightly soluble in water but easily dissolves in organic solvents like ethanol and diethyl ether [10]. Initially used in the early 20th century for manufacturing explosives and as an industrial chemical, 2,4-DNP was later found to promote weight loss by increasing metabolism and inducing fat burning. Despite its weight-loss potential, 2,4-DNP's severe toxic effects were quickly recognized since it interferes with cellular energy production, leading to hyperthermia, tachycardia, and, in many cases, death [11]. Due to its toxicity, 2,4-DNP was banned for human consumption by the Food and Drug Administration (FDA) in 1938 and by the UK's Food Agency in 2003. In 2015, Interpol issued a global alert highlighting its dangers [12,13]. Despite being a particularly dangerous substance [13,14], 2,4-DNP may be illegally added to weight loss products for its thermogenic effects. A recent analysis of social media posts revealed that the most commonly consumed dose was 150 mg (equivalent to 1-2 pills, depending on the formulation), followed by 300 mg (or 2-3 pills). Alarmingly, the lowest recorded lethal dose for humans was 4.3 mg kg^{-1}, while doses higher than 2.8 g have resulted in fatalities and generally associated with suicide attempts [15,16]. This underlines the extreme danger of using 2,4-DNP, where even small variations in dose can result in severe toxicity and death. Therefore, reliable and sensitive analysis methods for detecting 2,4-DNP are crucial for ensuring consumer safety. While chromatographic techniques performed at laboratories equipped with advanced and expensive equipment remain the gold standard as confirmatory techniques, there is also the need for fast, low-cost screening methods for checking potential adulteration of food supplements at point-of-care (e.g., customs). To date, electrochemical sensors developed for the detection of 2,4-dinitrophenol (2,4-DNP) have focused primarily on environmental monitoring, often requiring ultra-low detection limits due to the trace levels typically encountered in water samples. These systems commonly employ conventional electrodes modified with nanomaterials to enhance sensitivity, but are generally unsuitable for on-site use due to complexity and cost. In contrast, the presence of 2,4-DNP in food supplements—where it may be illicitly added in higher concentrations—demands simple, rapid, and cost-effective screening tools rather than ultra-sensitive detection. In this context, the present study introduces the first paper-based molecularly imprinted polymer (MIP) electrochemical sensor specifically designed for the detection of 2,4-DNP in food supplements. By combining the selectivity of MIPs with the affordability and portability of a paper-based platform, this work offers a promising solution for preliminary on-site screening, contributing to consumer safety and regulatory enforcement. In this context, Molecularly Imprinted Polymers (MIPs) represent a highly suitable approach for the selective recognition and determination of 2,4-DNP. These synthetic materials mimic biological recognition sites, offering high specificity, chemical stability, and reusability. When integrated with electrochemical transducers, MIPs enable rapid, cost-effective, and sensitive detection, making them particularly attractive for the development of robust chemical sensing platforms [17–22]. MIPs have been produced through various techniques, such as bulk polymerization, precipitation polymerization, sol-gel transformation, suspension polymerization, and in situ self-assembly electropolymerization [23,24]. Bulk polymerization is the most common and widely used method for MIP production because of its straightforward operation and low costs. However, bulk polymerization may have some shortcomings, such as the loss of binding sites during the mechanical disintegration of the synthesized polymer, which can lead to a lower yield and reduced sensor performance. The polymerization procedure in precipitation polymerization is similar to bulk polymerization, but with the advantage that post-treatment steps, such as grinding and sieving, are not required. This simplifies the process by reducing the number of steps and, more importantly, minimizes the risk of destroying the imprinted cavities, which are crucial for the sensor's selectivity. In precipitation polymerization, the reaction occurs in a large volume of organic solvent where the polymer is insoluble, causing it to precipitate. Unlike other methods, this approach does not require surfactants and allows control over the particle size [25,26].

In this study, to the best of our knowledge, we present the first paper-based MIP sensor designed for detecting 2,4-DNP in food supplements. The sensor was designed with a gold and carbon ink working electrode (WE), which provides enhanced conductivity and surface area. The MIP was synthesized through precipitation polymerization, ensuring robust formation of the MIP with selective recognition sites for 2,4-DNP. This paper-based platform offers several advantages, including low cost, ease of fabrication, and portability, making it highly suitable for on-site analysis in various settings. The optimization and performance of this sensor were evaluated, highlighting its potential for application in the determination of 2,4-DNP in food supplements.

2. Materials and methods

2.1. Reagents and solutions

2,4-DNP ($\geq$ 98 %), methacrylic acid (MAA), ethylene glycol dimethacrylate (EGDMA, 98 %), 2,2′-azobisisobutyronitrile (AIBN, $\geq$ 98 %), Nafion solution (perfluorinated resin solution, 5 wt.% in lower aliphatic alcohols and water), anhydrous N,N-dimethylformamide (DMF, $\geq$ 99.8 %), citric acid, potassium hexacyanoferrate(II) and (III), Chloroform (CHL, $\geq$ 99.0 %) and Toluene (TOL, $\geq$ 99.8 %) were obtained from Sigma-Aldrich. Methanol (MeOH, $\geq$ 99.9 %), acetonitrile (ACN, $\geq$ 99.5 %) 4-nitrophenol, and sodium benzoate were purchased from Riedel-de-Haën. Glacial acetic acid (AcOH, $\geq$ 99.8 %, VWR Chemicals), ethanol (EtOH, $\geq$ 99.5 % Carlo Erba), a zinc standard solution (Zn, Panreac), and phenol (Merck) were also used. The gold and silver inks used to fabricate the sensor's working, reference, and counter electrodes were obtained from Gwent Electronic Materials Ltd. Before use, MAA and EGDMA were purified by passing them through a short column filled with neutral alumina (Sigma-Aldrich) to remove inhibitors. All other reagents were of analytical grade and used without further purification. 2,4-DNP stock solutions were prepared daily in phosphate buffer (0.1 mol L^{-1}, pH = 7.0) and stored at 4°C. Ultrapure water (resistivity = 18.2 MΩ·cm) was obtained from a Millipore (Synergy UV) water purification system and used throughout the work. The food supplements were acquired online on different websites selling supplements for weight loss. In addition, food supplements, including different medicinal plants as ingredients, namely for boosting energy and improving mental performance and cognitive function, were also analyzed to evaluate possible matrix effects.

2.2. Apparatus and Measurements

Differential pulse voltammetric (DPV) and cyclic voltammetric (CV) measurements were performed using a Metrohm Autolab PGSTAT 204 potentiostat/galvanostat, equipped with a connector for screen-printed electrodes (Metrohm Dropsens) and connected to a computer running NOVA 1.10 software. All measurements were carried out at room temperature.

2.3. Fabrication of the electrochemical cell

A Fujifilm Dimatix Materials Printer inkjet printer (DMP-2850) equipped with a Samba piezoelectric printhead (12 nozzles) was used for the deposition of the electrodes on Toughprint waterproof paper. The

pattern was designed using Inkscape software, and both silver and gold conductive inks were printed with a resolution of 1693 dpi (drop spacing 15 μm). The electrodes were then sintered at 175°C for 10 minutes. After this, the electrochemical cells were cut into rectangles measuring 1 cm by 3 cm. The dimensions were chosen to match those of the screen-printed electrodes (SPE), allowing the use of the same connector. The working electrode (WE, ⌀ = 3 mm) was confined using an adhesive circle to prevent the spread of the drop. Subsequently, 3 μL of carbon ink (23% carbon paste in DMF) was drop-casted onto the working electrode and left to dry overnight. Finally, the adhesive circle around the working electrode was removed, and non-conductive adhesive tape was applied on top of the working electrode to prevent the solutions from spreading to the connections of the reference, auxiliary, and working electrodes (see Fig. 1).

2.4. MIP and NIP construction & Analytical signal recording

A schematic representation of the synthesis procedure, the sensor's construction, and the recording of the analytical signal is presented in Fig. 2. MIP microspheres for 2,4-DNP recognition were synthesized using precipitation polymerization. First, 1.0 mmol of 2,4-DNP and 4.0 mmol of MAA (functional monomer) were mixed in 15 mL of ACN. Next, 20 mmol of EGDMA (crosslinker) and 0.30 mmol of AIBN (initiator) were added to the mixture, which was then purged with nitrogen for 10 min. The mixture was subsequently heated at 60°C in a thermoblock for 4 h. The resulting mixture was centrifuged, and the MIP was separated from the reaction medium by filtration. 2,4-DNP was removed from the MIP by repeated washing with a mixture of AcOH and MeOH (1:9, v/v). Finally, the polymer was collected and dried in an oven at 60°C. A non-imprinted polymer (NIP) was synthesized using the same procedure, without the use of 2,4-DNP. After synthesizing the polymeric MIP/NIP microspheres, 5 mg of the material was weighed and dispersed in a mixture of 300 μL of EtOH, 790 μL of phosphate buffer (0.1 mol L^{-1}, pH = 7.0), and 10 μL Nafion. The mixture was then sonicated for 5 min and 2 μL of the prepared suspension was deposited onto the WE of each electrochemical cell and allowed to dry at room temperature. This procedure was repeated 6 times.

To obtain the analytical signals, 40μL aliquots of either standard or sample solutions were placed on the paper-based cell, covering the three electrodes. Differential pulse voltammograms (DPVs) were recorded by applying a potential between 0.2 and 1.4 V (pulse amplitude: 50 mV; scan-rate: 50 mV s^{-1}). For the MIP/NIP characterization, 40 μL of a 1 mmol L^{-1} $[Fe(CN)_6]^{3-/4-}$ solution was dropped onto the electrochemical cell. Cyclic voltammograms (CVs) were recorded by applying a potential between -0.1 and 0.6 V (scan-rate: 50 mV s^{-1}). Each sensor was used only once.

2.5. Sample preparation

Samples of food supplements intended for energy boost/metabolism and weight loss were analysed. The samples were prepared using the following procedure: 6 mg of the capsule contents or crushed pill were weighed and 2000 μL of phosphate buffer (0.1 mol L^{-1}, pH = 7.0) were added. The mixture was then sonicated for 15 min and stored at 4°C.

3. Results and discussion

3.1. MIP and NIP characterization

Before proceeding with the characterization of the MIP and NIP-modified sensors, preliminary tests were carried out to confirm the electrochemical functionality of the fabricated paper-based platform. For this purpose, differential pulse voltammetry (DPV) measurements were performed in the presence of 2,4-DNP using both the paper-based sensor and a conventional screen-printed carbon electrode (SPCE). As shown in Fig. S1, both platforms exhibited comparable electrochemical responses at a DNP concentration of 1000 μmol L^{-1}, validating the capability of the paper-based transducer to support electrochemical measurements. Furthermore, in the absence of the MIP layer, the paper-based sensor did not generate a detectable signal when exposed to 500 μmol L^{-1} DNP. However, after MIP modification, a well-defined peak was observed, as will be further discussed in the following sections. These preliminary results validate the suitability of the paper-based platform for subsequent molecular imprinting and selective detection of DNP.

The electrochemical characterization of the different steps involved in MIP/NIP sensor fabrication was carried out using cyclic voltammetry (CV). The redox behaviour of the $[Fe(CN)_6]^{3-/4-}$ probe served as an indicator of the sensor's electron transfer capability throughout the

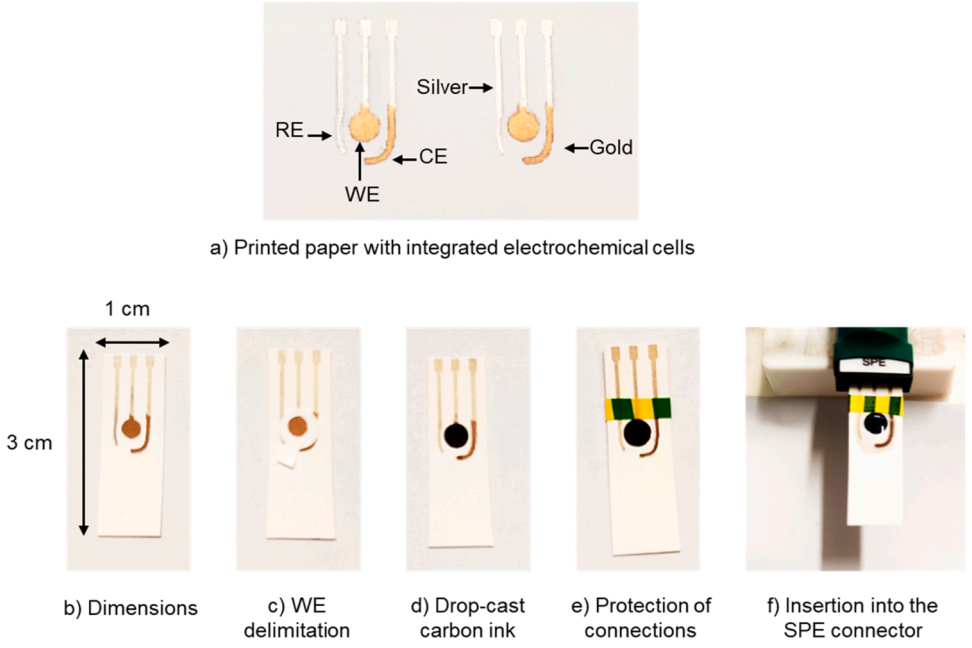

Fig. 1. Photographs of a) the front view of the electrochemical cell; b to e) different construction steps of the electrochemical cell, and f) the placement of the electrochemical cell into the SPE connector.

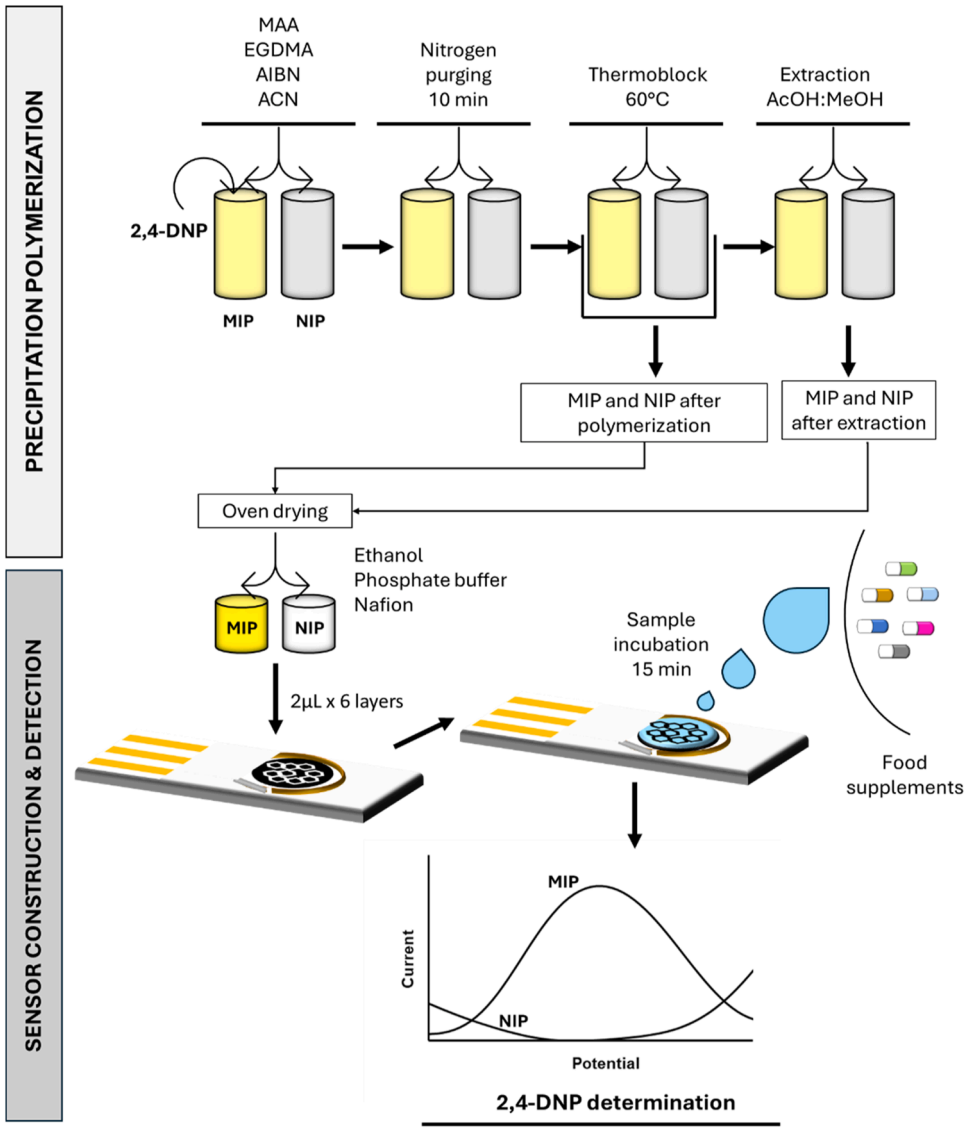

Fig. 2. Schematic representation of the MIP/NIP synthesis via precipitation polymerization, followed by the preparation of the electrochemical cell through the deposition of 6 layers of MIP/NIP microspheres. The detection process was then carried out using differential pulse voltammetry (DPV).

modification process. Fig. 3 displays the CV voltammograms corresponding to the redox reaction of $[Fe(CN)_6]^{3-/4-}$ for the MIP (Fig. 3A) and NIP (Fig. 3B). Initially, a typical reversible redox process is observed for the unmodified (bare) electrode, characterized by well-defined redox peaks and a relatively high peak current (ip). However, after the deposition of six layers of MIP or NIP polymers onto the working electrode (WE), a marked decrease in current response was detected, indicating the successful immobilization of a compact polymeric film that hinders the charge transfer of the redox probe, effectively covering the electrode surface. Following template extraction in the MIP, a slight increase in peak current was observed, which is attributed to the formation of specific cavities within the polymer matrix, facilitating partial access of the redox species to the WE surface. Upon incubation with a 500 µmol L^{-1} 2,4-DNP solution, a further decrease in ip was noted, confirming the rebinding of 2,4-DNP molecules into the imprinted cavities, thus limiting electron transfer due to steric and electrostatic effects. In addition to the variations in current intensity, slight shifts in peak potentials were also observed, particularly after incubation with the target analyte. These shifts are indicative of alterations in the interfacial electron transfer kinetics and local microenvironment caused by the binding of 2,4-DNP within the MIP layer. Such shifts were notably more pronounced in the MIP than in the NIP, reinforcing the evidence of selective recognition. In contrast, the NIP electrode showed minimal changes in both current response and peak potentials throughout the process, consistent with the absence of specific recognition sites. These results highlight the selectivity and functionality of the developed MIP sensor, as the NIP serves as an essential control to distinguish between specific and non-specific interactions.

3.2. *Optimization steps*

A key aspect in the optimization of molecularly imprinted polymers is understanding the recognition mechanism that governs selective binding. This mechanism is directly influenced by the interactions established during polymerization, as well as by the efficiency of template removal. The recognition mechanism of the synthesized MIP relies on the formation of specific binding sites complementary to the template molecule in size, shape, and functional groups. Methacrylic acid (MAA) was used as the functional monomer due to its ability to form non-covalent interactions (e.g., hydrogen bonding) with the template during the pre-polymerization phase. Acetonitrile, as a porogenic solvent, favored these interactions by minimizing solvent interference. Upon

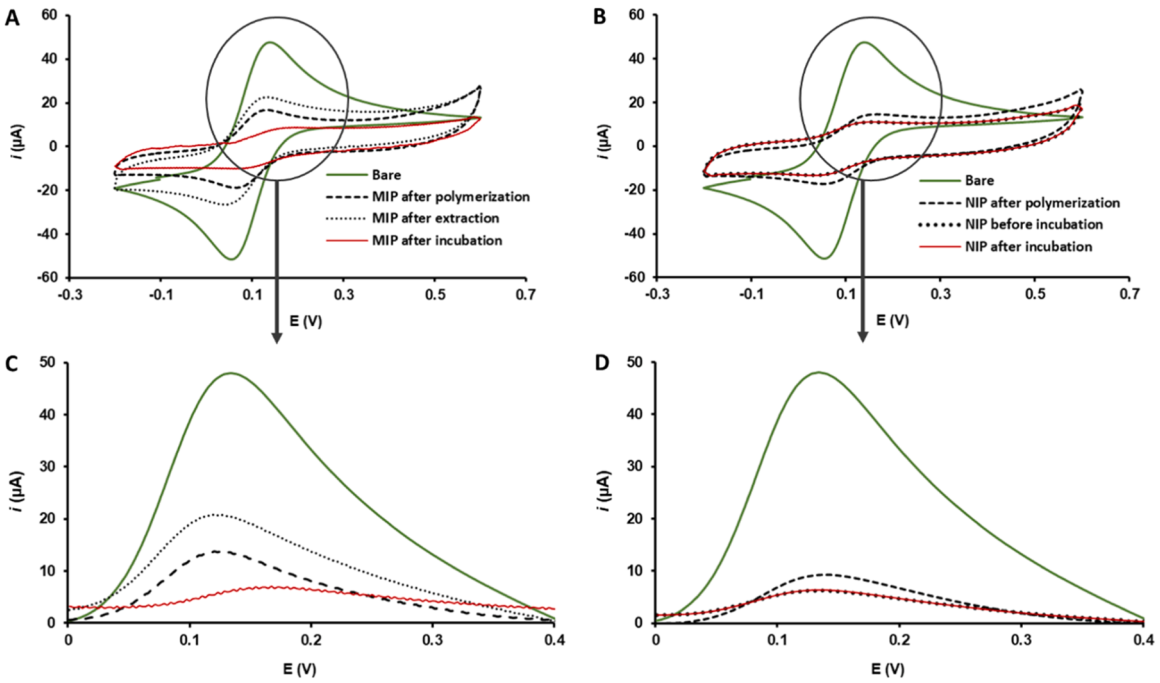

Fig. 3. Characterization of the MIP and NIP sensors using cyclic voltammetry (CV), highlighting the enlargement of the anodic peak of the $[Fe(CN)_6]^{3-/4-}$ redox system, in the presence of 1 mmol L^{-1} $[Fe(CN)_6]^{3-/4-}$ solution. (A) CVs of the bare sensor, MIP after polymerization, after template extraction, and after incubation with 500 μmol L^{-1} 2,4-DNP; (B) CVs of the bare sensor and NIP at the same preparation stages; (C) Enlarged view of the anodic peak shown in (A) and (D) Enlarged view of the anodic peak shown in (B).

initiation by AIBN, free radical polymerization was carried out with ethylene glycol dimethacrylate (EGDMA) as the crosslinker, forming a rigid polymer matrix that preserved the spatial arrangement of the template–monomer complexes. After polymerization, the template molecule was removed by washing the polymer with a solution of acetic acid and methanol, a procedure repeated over 4 days with the extraction solution being renewed three times per day to ensure efficient and complete removal of the template. This mixture effectively disrupted the non-covalent interactions—such as hydrogen bonds and electrostatic forces—between the polymer and the template, allowing for complete removal without affecting the integrity of the imprinted sites. Acetic acid was chosen for its ability to donate protons, weakening hydrogen bonds, while methanol, a polar protic solvent, aids in solubilizing and extracting the template from the polymer matrix. As a result, highly

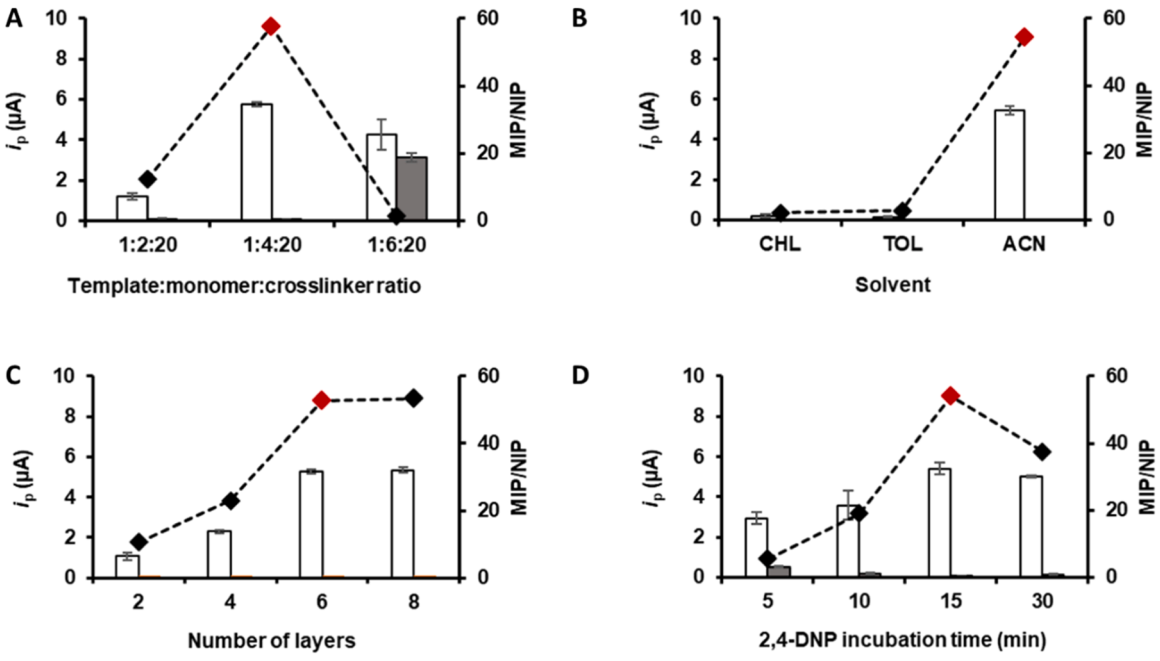

Fig. 4. Influence of various experimental parameters on i_p and MIP/NIP ratio. **(A)** Optimization of the template:monomer:crosslinker ratio (1:2:20, 1:4:20, and 1:6:20); **(B)** Effect of different solvents (chloroform, toluene, and acetonitrile); **(C)** Impact of the number of layers (2, 4, 6, and 8) deposited on the WE; **(D)** Effect of 2,4-DNP incubation time (5, 10, 15, and 30 min) on the WE. Experimental conditions: NIP (500 μmol L^{-1}, dark grey bars) and MIP (2,4-DNP 500 μmol L^{-1}, white bars). Results are presented as average ± standard deviation (n = 3).

specific recognition cavities remained within the polymer matrix. These cavities, being chemically and structurally complementary to the original template, enable selective rebinding of the target molecule, thus conferring the MIP its molecular recognition ability. In this way, several key parameters influencing the sensor's performance were investigated to optimize the imprinting process: (a) the template:monomer:crosslinker ratio, (b) the solvent, (c) the number of layers deposited on the WE, and (d) the incubation time of 2,4-DNP. Optimization studies were performed, and the final parameters were selected based on the relationship between MIP/NIP, ensuring enhanced selectivity and sensitivity for the determination of 2,4-DNP. This was determined by comparing the responses of the MIP and NIP sensor in the presence of 500 μmol L^{-1} 2,4-DNP (incubation step). The results of these optimizations are shown in Fig. 4. As shown in Fig. 4A, different template: monomer ratios were tested while maintaining a constant amount of crosslinker. An increase in i_p and MIP/NIP ratio was observed between 1:2:20 and 1:4:20 ratios, followed by a decrease beyond this point. This can be attributed to fewer interactions between the monomer and the template molecule. This can lead to fewer specific interactions between the analyte and the recognition sites, as the monomer may not be as effectively aligned or positioned to form selective cavities for the analyte. The 1:4:20 ratio was selected as it provided the highest i_p and MIP/NIP ratio, which is likely due to an optimal balance between the number of available binding sites and the structural integrity of the polymer matrix. Various solvents, including CHL, TOL, and ACN, were evaluated (Fig. 4B). The use of CHL and TOL resulted in very low i_p values and MIP/NIP ratios, possibly due to the poor solubility of 2,4-DNP in these solvents or limited affinity between the template and the monomer in them. ACN, however, produced a significantly better results, suggesting it offers better solvation of the template and facilitates more efficient interaction between the template and the monomer. Consequently, ACN was chosen as the solvent for the synthesis of the MIP. Fig. 4C illustrates the effect of the number of MIP layers deposited on the WE. An increase of i_p and MIP/NIP ratio was observed from 2 to 6 layers, after which they plateaued. Six layers were ultimately chosen, as this number provided the sensor with a greater number of binding sites without compromising the signal, potentially enhancing the sensor's sensitivity. As indicated in Fig. 4D, an incubation time of 15 min was identified as ideal for 2,4-DNP binding to the available sites. After 30 min of incubation, a slight decrease of the i_p value and the MIP/NIP ratio was observed, which is possibly due to the saturation of the binding sites or the desorption of the analyte, which can occur if the incubation time is too long. After each incubation step, the electrodes were rinsed with ultrapure water to remove any unbound or non-specifically adsorbed compounds, ensuring that only the analyte retained in the specific cavities contributed to the final electrochemical response.

3.3. Electroanalytical performance of the sensor

Using the optimized conditions of the paper-based sensor, 2,4-DNP solutions with concentrations between 50 and 1000 μmol L^{-1} were analysed. Representative voltammograms for this concentration range obtained with the MIP sensor are shown in Fig. 5A, with a more detailed view provided in Fig. 5B. In Fig. 5C, it is possible to observe peak intensities of 14.4 ± 0.3 μA for MIP, 0.60 ± 0.05 μA for NIP, and no signal for the bare electrode when incubated with 2,4-DNP at a concentration of 1000 μmol L^{-1}, which corresponds to the higher concentration in the calibration plot. This suggests that the MIP exhibits a strong recognition ability for 2,4-DNP, leading to a significantly higher signal compared to the non-imprinted polymer (NIP) and the bare electrode, which shows negligible interaction with the analyte. The calibration plot for both the MIP- and NIP-sensors are presented in Fig. 5D. A linear relationship between i_p and 2,4-DNP concentration for the MIP sensor was established, following the equation: i_p (μA) = 0.0148 [2,4-DNP] (μmol L^{-1}) - 0.788, with an excellent correlation coefficient (r = 0.999). The analytical figures of merit can be found in Table S1. Additionally, a linear relationship between the peak current (ip) and 2,4-DNP was observed for the NIP sensor, following the equation:: i_p (μA) = 0.0005 [2,4-DNP] (μmol L^{-1}) – 0.1099. However, the low correlation coefficient (r = 0.821) and the low slope suggests limited specificity of the sensor for 2,4-DNP detection. The limits of detection (LOD, 16.3 μmol L^{-1}) and quantification (LOQ, 54.2 μmol L^{-1}) were determined based on the calibration data using the equations LOD = $3S_b/m$ and LOQ=$10S_b/m$ (S_b represents the standard deviation of the blank and m is the slope of the

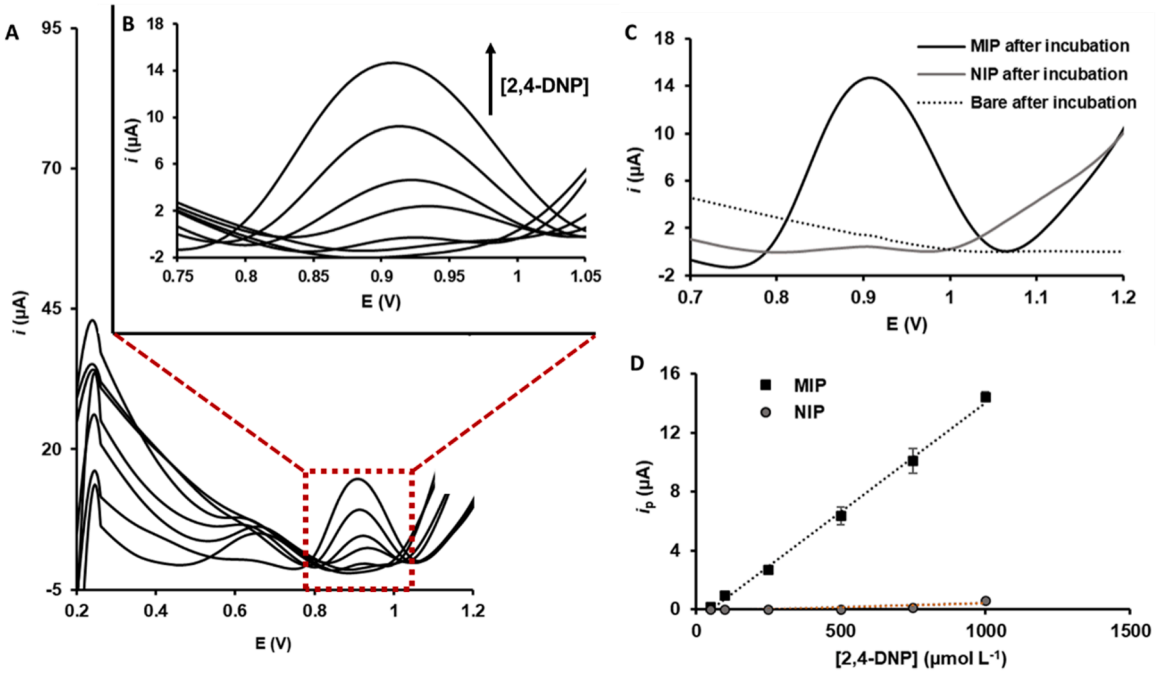

Fig. 5. **(A)** DPV voltammograms of the paper-based MIP sensor for 50 to 1000 μmol L^{-1} 2,4-DNP solutions. **(B)** Enlarged view of the DPV voltammograms. **(C)** DPV voltammograms of the paper-based MIP, NIP, and bare electrode upon incubation with a 1000 μmol L^{-1} 2,4-DNP solution. **(D)** Calibration plots for the MIP- and NIP sensors. Results are presented as average ± standard deviation (n = 3).

calibration straight). This indicates the sensor's capability to detect and quantify low concentrations of 2,4-DNP. These levels are crucial considering the potential health risks associated with the illicit presence of 2,4-DNP in food supplements. The sensor's LOD corresponds to 0.003 g L^{-1} and, given that reported fatal doses range from 2.8 g to approximately 5 g, this demonstrates its usefullness for safety monitoring of food supplements. The method showed good precision (coefficient of variation (V_{x0}) of 5.2 %). The precision of the results was assessed through three successive measurements (repeatability) and through the analysis on three separate days (reproducibility), using different paper-based sensors, of a 500 μmol L^{-1} 2,4-DNP solution. The average coefficients of variation (CV) were 1.9 % for repeatability and 3.9 % for reproducibility, inicating that the MIP sensor offers precise results, confirming its reliability for analytical applications. Although no experimental stability tests were performed in this study, it is important to note that the MIP sensor does not rely on biological recognition elements such as enzymes or antibodies, which are typically prone to degradation. Due to the inherently stable nature of the synthetic polymer matrix, MIPs are known for their chemical and thermal robustness, suggesting that the sensor is likely to exhibit good long-term stability under appropriate storage and operational conditions.

3.4. Selectivity and Interference studies

To assess the selectivity of the MIP sensor toward 2,4-DNP, several ingredients that are commonly present in nutritional supplements were tested: sodium benzoate, 4-nitrophenol, zinc, citric acid, and phenol.

The selection of interferents for the selectivity study was based on their common occurrence in food supplements, either as preservatives, metallic components, flavoring agents, or potential contaminants. Sodium benzoate and citric acid are widely used as preservatives and acidulants in food supplements. Zinc is frequently included as a trace element in multivitamin and mineral supplements. Phenol and 4-nitrophenol were selected as structurally related analogues to 2,4-DNP, sharing similar aromatic characteristics and hydroxyl or nitro substitutions, potentially interfering with molecular recognition. 4-nitrophenol, in particular, has been occasionally reported as a degradation product or impurity in synthetic compounds and was included to assess the sensor's selectivity under realistic conditions. Thus, solutions of these ingredients and 2,4-DNP (control) (all at 500 μmol L^{-1}) were analysed individually and in a combined solution (Fig. 6). Additionally, a mixture containing all of them and 2,4-DNP (all at 500 μmol L^{-1}) was analysed to assess their interference in the analysis. As can be seen in Fig. 6, none of the tested ingredients produced an analytical signal when tested alone or in the mixture, indicating that they do not interact with or bind to the specific recognition sites designed for 2,4-DNP on the MIP sensor. This confirms the sensor's selectivity, which is crucial for the reliable detection of 2,4-DNP in complex matrices, reducing the likelihood of false positives due to non-specific binding. For the mixture containing all the ingredients and 2,4-DNP, the current response was 5.72 ± 0.16 μA, which is comparable to the response obtained for the MIP with 2,4-DNP at 500 μmol·L^{-1} (6.04 ± 0.47 μA). This demonstrates that the tested species do not interfere with the analytical performance of the sensor.

3.5. Sample analysis

To assess the practicality of the paper-based sensor for determining 2,4-DNP in food supplements, capsules and pills marketed for energy boost, metabolism enhancement, mental performance, and weight loss were analysed. The quantification of 2,4-DNP was carried out by recording voltammograms before and after spiking the extracts with known amounts of 2,4-DNP at two different concentrations. The voltammograms recorded before spiking exhibited no oxidation peak, indicating that the amount of 2,4-DNP in the tested samples was below the LOD. To evaluate the sensor's response, two different concentrations of 2,4-DNP were spiked into each sample. Since recovery values between 85% and 107% were obtained, the samples tested for weight loss were spiked with only one concentration of 2,4-DNP.

Following the spiking of the weight loss extracts with a concentration of 250 μmol L^{-1} of 2,4-DNP, recovery values between 85.9 % and 108.3 %, with coefficients of variations below 10 %, were obtained (Table 1). These results demonstrate not only the sensor's accuracy but also its capability for precise quantification of 2,4-DNP in complex matrices such as food supplement extracts. This indicates the sensor's robustness and reliability, making it a suitable tool for routine monitoring of 2,4-DNP in food supplements to ensure consumer safety and product compliance.

As far as we are aware, this is the first MIP-paper-based sensor for the determination of 2,4-DNP in food supplements. Previous studies have typically employed conventional transducers such as glassy carbon electrodes (GCE) [22,27] or graphite-epoxy composites [28], often modified with conductive nanomaterials like graphene oxide (GO) [27] or nickel–GO composites [22], to enhance sensitivity. These approaches (Table S2) have yielded low limits of detection and narrow linear ranges, particularly suitable for environmental applications—such as in surface or wastewater—where 2,4-DNP is present at trace levels and strict safety and environmental regulations necessitate ultra-sensitive detection. However, the context of food supplements differs substantially. In such products, 2,4-DNP is usually present at significantly higher concentrations due to its deliberate and illicit addition as a weight-loss agent. Therefore, the need for extremely low LODs is less critical. In this regard, although the sensor developed in this work exhibits a higher LOD compared to previously reported MIP-based electrochemical platforms, it offers unique and relevant advantages. Most notably, it represents the first example of a MIP integrated onto a disposable, low-cost

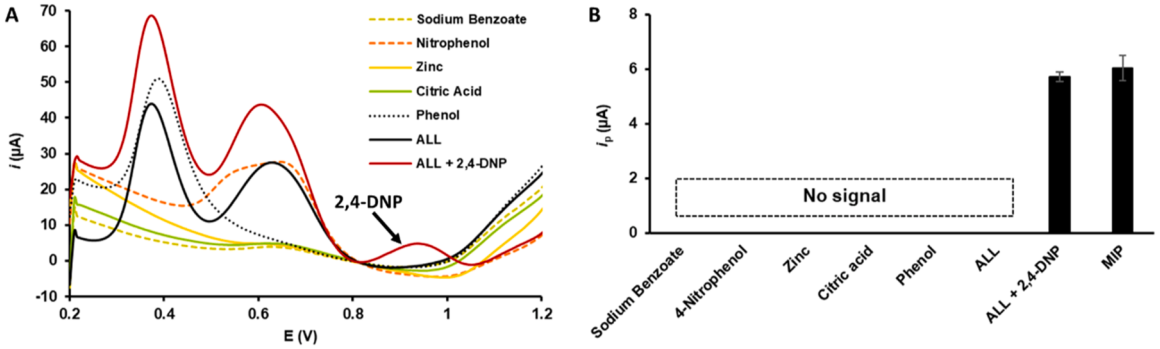

Fig. 6. Selectivity and interference studies. **(A)** DPV voltammograms of the MIP sensor for individual solutions of sodium benzoate, 4-nitrophenol, zinc, citric acid, phenol, and their mixture (ALL) at 500 μmol L^{-1}, as well as the mixture of these species with 2,4-DNP (ALL+2,4-DNP, all at 500 μmol L^{-1}). **(B)** i_p values for each solution. Results are presented as average ± standard deviation (n = 3).

Table 1
Results of the recovery tests for the quantification of 2,4-DNP in food supplements samples. Results are presented as average ± standard deviation (n = 3).

Food supplement	Purpose	2,4-DNP added (μmol L^{-1})	2,4-DNP found (μmol L^{-1})	Recovery (%)
A	To support normal energy-yielding metabolism and help reduce tiredness and fatigue	**350**	315.3 ± 27.1	90.1 ± 7.7
		450	413.0 ± 26.7	91.8 ± 5.9
B	Mental performance and Energy	**100**	111.7 ± 6.5	106.6 ± 7.2
		650	641.5 ± 25.2	98.7 ± 3.9
C	Cognitive function and peripheral circulation	**250**	226.3 ± 13.4	90.5 ± 5.4
		900	875.3 ± 43.9	97.3 ± 4.9
D	Energy	**100**	85.2 ± 2.5	85.2 ± 2.5
		400	380.0 ± 18.4	95.0 ± 4.6
E	Weight loss (slimming activateur, fat burner, thermoshape)	**250**	235.1 ± 3.1	94.0 ± 3.1
F			270.8 ± 12.5	108.3 ± 5.0
G			230.3 ± 7.4	92.1 ± 3.0
H			214.8 ± 0.8	87.8 ± 0.3
I			219.6 ± 0.8	85.9 ± 0.3
J			220.9 ± 25.7	88.4 ± 10.3
K			250.6 ± 9.3	100.2 ± 3.7
L			258.6 ± 11.3	103.5 ± 4.5

paper-based electrode specifically designed for 2,4-DNP detection in food supplements. Furthermore, while the use of advanced nanomaterials in earlier studies contributed to lower detection limits, they often involve complex fabrication steps, increased costs, and reduced compatibility with point-of-need applications. In contrast, the proposed platform favors simplicity, sustainability, and affordability—features that are crucial for rapid, on-site screening. Importantly, the method demonstrated acceptable recoveries in a complex food supplement matrix, supporting its practical utility for preliminary screening and routine monitoring, where portability and ease of use are as critical as analytical performance.

4. Conclusions

In this study, a paper-based MIP sensor was successfully developed for the selective and sensitive determination of 2,4-DNP in food supplements. The optimization of key parameters, including the template: monomer:crosslinker ratio, solvent, number of MIP layers, and incubation time, resulted in a sensor with a broad linear range (50 to 1000 μmol L^{-1}) and low limits of detection and quantification (16.3 μmol L^{-1} and 54.2 μmol L^{-1}, respectively). The paper-based sensor exhibited good precision, with low coefficients of variation for both inter-electrode and inter-day tests, indicating consistent analytical performance. The recovery tests further confirmed the sensor's accuracy and reliability in real sample analysis, achieving recovery rates above 85 % with RSD values below 10 %, even in complex matrices. The sensor demonstrated high selectivity for 2,4-DNP.

Given its affordability, rapid response, and ease of use, this sensor offers a promising tool for the decentralized and routine monitoring of 2,4-DNP in food supplements. This is particularly important considering the potential health risks associated with the illicit use of 2,4-DNP in weight loss products. The developed MIP sensor provides an efficient means to ensure consumer safety and product compliance, contributing to the overall quality control of food supplements on the market.

Funding

This work received financial support from the European Union (FEDER funds through COMPETE POCI-01-0145-FEDER-030735) and Portuguese National Funds (Fundação para a Ciência e a Tecnologia (FCT)) through the project PTDC/SAU-PUB/3803/2021 – POIROT (https://doi.org/10.54499/PTDC/SAU-PUB/3803/2021). This work also received financial support from PT national funds (FCT/MECI, Fundação para a Ciência e a Tecnologia / Ministério da Educação, Ciência e Inovação) through the project UID/50006 - Laboratório Associado para a Química Verde - Tecnologias e Processos Limpos.

CRediT authorship contribution statement

Ricarda Torre: Writing – original draft, Investigation, Formal analysis, Data curation. **Patrícia Rebelo:** Supervision, Methodology, Investigation, Formal analysis, Data curation, Conceptualization. **Isabel Seguro:** Writing – original draft, Visualization, Investigation, Formal analysis. **João G. Pacheco:** Writing – review & editing, Validation, Supervision, Resources, Methodology, Funding acquisition, Conceptualization. **Joana S. Amaral:** Writing – review & editing, Validation, Project administration, Funding acquisition. **Henri P.A. Nouws:** Writing – review & editing, Supervision, Resources, Project administration, Methodology, Funding acquisition, Conceptualization. **Cristina Delerue-Matos:** Writing – review & editing, Resources, Project administration, Funding acquisition.

Declaration of competing interest

The authors declare that they have no known competing financial interests or personal relationships that could have appeared to influence the work reported in this paper.

Acknowledgements

João Pacheco is thankful for his contract (2023.07458.CEECIND/CP2842/CT0002) financed by FCT/Ministério da Ciência, Tecnologia e Ensino Superior (MCTES) - CEEC Individual Program Contract. Patrícia Rebelo is grateful for her grant from the FCT-funded project PaperSenseMIP (PTDC/QUI-QAN/3899/2021, https://doi.org/10.54499/PTDC/QUI-QAN/3899/2021). Isabel Seguro thanks FCT and ESF (European Social Fund) through POCH (Programa Operacional Capital Humano) for her PhD grant (2022.12344.BD, https://doi.org/10.54499/2022/12344/BD). This work received support and help from the FCT/MCTES funded project PaperSenseMIP (PTDC/QUI-QAN/3899/2021, https://doi.org/10.54499/PTDC/QUI-QAN/3899/2021). through national funds.

Supplementary materials

Supplementary material associated with this article can be found, in the online version, at doi:10.1016/j.electacta.2025.147177.

Data availability

Data will be made available on request.

References

[1] M. Shahbaz Alam, N. Khandale, D. Birla, S. Vishwas, B. Bashir, M.V.N.L. Chaitanya, G. Gupta, A. Patel, S. Patel, T. Collet, K. Dua, S.Kumar Singh, Harnessing the role of

analytical techniques in analysis of adulterants in dietary supplements, Microchem. J. 202 (2024) 1–9, https://doi.org/10.1016/j.microc.2024.110786.
[2] E. Mah, O. Chen, D.J. Liska, J.B. Blumberg, Dietary Supplements for Weight Management: A Narrative Review of Safety and Metabolic Health Benefits, Nutrients. 14 (2022) 1–23, https://doi.org/10.3390/nu14091787.
[3] T. Rocha, J.S. Amaral, M.B.P.P. Oliveira, Adulteration of Dietary Supplements by the Illegal Addition of Synthetic Drugs: A Review, Compr. Rev. Food Sci. Food Saf. 15 (2016) 43–62, https://doi.org/10.1111/1541-4337.12173.
[4] European Commission, Directive 2002/46/EC of the European Parliament and of the council of 10 June 2002 on the approximation of the laws of the member states relating to food supplements, 2002.
[5] US Food and Drug Administration (FDA), Dietary Supplements, Https://Www.Fda.Gov/Food/Dietary-Supplements (accessed in April 2025).
[6] N.M. Reeuwijk, B.J. Venhuis, D. de Kaste, R.L.A.P. Hoogenboom, I.M.C.M. Rietjens, M.J. Martena, Active pharmaceutical ingredients detected in herbal food supplements for weight loss sampled on the Dutch market, Food Additives & Contaminants: Part A: Chemistry, Analysis, Control, Exposure & Risk Assessment 31 (2014) 1783–1793, https://doi.org/10.1080/19440049.2014.958574.
[7] D.B. da, J. Neves, E.D. Caldas, Determination of caffeine and identification of undeclared substances in dietary supplements and caffeine dietary exposure assessment, Food and Chemical Toxicology 105 (2017) 194–202, https://doi.org/10.1016/j.fct.2017.03.063.
[8] C.M. White, Continued Risk of Dietary Supplements Adulterated With Approved and Unapproved Drugs: Assessment of the US Food and Drug Administration's Tainted Supplements Database 2007 Through 2021, J. Clin. Pharmacol. 62 (2022) 928–934, https://doi.org/10.1002/jcph.2046.
[9] M. Amidžić, J. Banović Fuentes, J. Banović, L. Torović, Notifications and Health Consequences of Unauthorized Pharmaceuticals in Food Supplements, Pharmacy 11 (2023) 154, https://doi.org/10.3390/pharmacy11050154.
[10] Y.D. Ivanov, K.A. Malsagova, T.O. Pleshakova, R.A. Galiullin, A.F. Kozlov, I. D. Shumov, I.A. Ivanova, A.I. Archakov, V.P. Popov, A.V. Latyshev, K.V. Rudenko, A.V. Glukhov, Ultrasensitive detection of 2,4-dinitrophenol using nanowire biosensor, J. Nanotechnol. 2018 (2018) 1–6, https://doi.org/10.1155/2018/9549853.
[11] B. Singh, A. Singh, A. Sharma, P. Mahajan, S. Verma, B. Padha, A. Ahmed, S. Arya, Electrochemical sensing and photocatalytic degradation of 2,4-dinitrophenol via bismuth (III) oxide nanowires, J. Mol. Struct. 1255 (2022) 1–10, https://doi.org/10.1016/j.molstruc.2022.132379.
[12] S. Ko, S. Gunasekaran, J. Yu, Self-indicating nanobiosensor for detection of 2,4-dinitrophenol, Food Control 21 (2010) 155–161, https://doi.org/10.1016/j.foodcont.2009.05.006.
[13] D. Sousa, H. Carmo, R. Roque Bravo, F. Carvalho, M. de L. Bastos, P. Guedes de Pinho, D. Dias da Silva, Diet aid or aid to die: an update on 2,4-dinitrophenol (2,4-DNP) use as a weight-loss product, Arch. Toxicol. 94 (2020) 1071–1083, https://doi.org/10.1007/s00204-020-02675-9.
[14] T. Ekar, S. Kreft, Common risks of adulterated and mislabeled herbal preparations, Food and Chemical Toxicology 123 (2019) 288–297, https://doi.org/10.1016/j.fct.2018.10.043.
[15] D.J. Germain, D.C. Leavey, P.M.C. Van Hout, P.J. McVeigh, 2,4 dinitrophenol: It's not just for men, International Journal of Drug Policy 95 (2021) 1–7, https://doi.org/10.1016/j.drugpo.2020.102987.
[16] Ž. Jakopin, Risks associated with fat burners: A toxicological perspective, Food and Chemical Toxicology 123 (2019) 205–224, https://doi.org/10.1016/j.fct.2018.10.051.
[17] L. Jia, Y. Mao, S. Zhang, H. Li, M. Qian, D. Liu, B. Qi, Electrochemical switch sensor toward ephedrine hydrochloride determination based on molecularly imprinted polymer/nafion-MWCNTs modified electrode, Microchem. J. 164 (2021) 1–8, https://doi.org/10.1016/j.microc.2021.105981.
[18] K. Kor, K. Zarei, Development and characterization of an electrochemical sensor for furosemide detection based on electropolymerized molecularly imprinted polymer, Talanta 146 (2016) 181–187, https://doi.org/10.1016/j.talanta.2015.08.042.
[19] A. Nezhadali, M. Mojarrab, Computational study and multivariate optimization of hydrochlorothiazide analysis using molecularly imprinted polymer electrochemical sensor based on carbon nanotube/polypyrrole film, Sens. Actuat., B Chem. 190 (2014) 829–837, https://doi.org/10.1016/j.snb.2013.08.086.
[20] B. Deiminiat, G.H. Rounaghi, M.H. Arbab-Zavar, Development of a new electrochemical imprinted sensor based on poly-pyrrole, sol–gel and multiwall carbon nanotubes for determination of tramadol, Sens. Actuat., B Chem. 238 (2017) 651–659, https://doi.org/10.1016/j.snb.2016.07.110.
[21] Q. Hao, L. Lu, X. Kan, Probe and analogue: Double roles of thionine for aloe-emodin selective and sensitive ratiometric detection, Sens. Actuat., B Chem. 292 (2019) 247–253, https://doi.org/10.1016/j.snb.2019.04.129.
[22] T. Jing, H. Xia, J. Niu, Y. Zhou, Q. Dai, Q. Hao, Y. Zhou, S. Mei, Determination of trace 2,4-dinitrophenol in surface water samples based on hydrophilic molecularly imprinted polymers/nickel fiber electrode, Biosens. Bioelectron. 26 (2011) 4450–4456, https://doi.org/10.1016/j.bios.2011.05.001.
[23] N. Zalpour, M. Roushani, A polydopamine imprinted array on a binder-free carbon cloth assembled by gold carbon quantum dots as a portable flexible 3D nano-electrochemical sensor for selective trace monitoring of orlistat (xenical), Microchem. J.l 190 (2023), https://doi.org/10.1016/j.microc.2023.108750.
[24] A. Adumitrăchioaie, M. Tertiş, A. Cernat, R. Săndulescu, C. Cristea, Electrochemical methods based on molecularly imprinted polymers for drug detection. A review, Int. J. Electrochem. Sci. 13 (2018) 2556–2576, https://doi.org/10.20964/2018.03.75.
[25] P. Rebelo, E. Costa-Rama, I. Seguro, J.G. Pacheco, H.P.A. Nouws, M.N.D. S. Cordeiro, C. Delerue-Matos, Molecularly imprinted polymer-based electrochemical sensors for environmental analysis, Biosens. Bioelectron. 172 (2021) 1–18, https://doi.org/10.1016/j.bios.2020.112719.
[26] T. Sajini, B. Mathew, A brief overview of molecularly imprinted polymers: Highlighting computational design, nano and photo-responsive imprinting, Talanta Open. 4 (2021) 1–20, https://doi.org/10.1016/j.talo.2021.100072.
[27] Y. Liu, L. Zhu, Y. Zhang, H. Tang, Electrochemical sensoring of 2,4-dinitrophenol by using composites of graphene oxide with surface molecular imprinted polymer, Sens. Actuat., B Chem. 171–172 (2012) 1151–1158, https://doi.org/10.1016/j.snb.2012.06.054.
[28] A. Herrera-Chacon, A. Gonzalez-Calabuig, M. Del Valle, Dummy molecularly imprinted polymers using dnp as a template molecule for explosive sensing and nitroaromatic compound discrimination, Chemosensors 9 (2021) 1–15, https://doi.org/10.3390/chemosensors9090255.